JOURNAL OF STRUCTURAL BIOLOGY 108, 148–161 (1992)

Glial Fibrillary Acidic Protein and Its mRNA: Ultrastructural Detection and Determination of Changes after CNS Injury

PAGE A. ERICKSON, STUART C. FEINSTEIN, GEOFFREY P. LEWIS, AND STEVEN K. FISHER

Neuroscience Research Institute and the Department of Biological Sciences, University of California, Santa Barbara, California 93106

Received September 9, 1991, and in revised form January 9, 1992

We have previously demonstrated that glial fibrillary acidic protein (GFAP) containing intermediate filaments in retinal Müller cells undergo both quantitative induction and subcellular reorganization as a response to long-term retinal detachment (an induced CNS degeneration wherein the Müller cells form a multicellular scar). This study demonstrates by RNA blotting analysis that normal retina expresses a low basal level of GFAP mRNA, which is induced approximately 500% within 3 days of retinal detachment. At the cellular level, electron microscopic *in situ* hybridization analysis readily detects GFAP mRNA in Müller cells of detached retinas, but not in normal retinas. On the other hand, GFAP mRNA was readily detected in retinal astrocytes (which appear to express GFAP mRNA at high, constitutive levels). In both cell types, the ultrastructural localization of GFAP mRNA was the same. In the nuclei, the GFAP mRNA was associated with amorphous, electron-dense regions within the euchromatin. In the cytoplasm, the GFAP mRNA was associated with intermediate filaments near the nuclear pores, along the filaments when no other structures were apparent, and when the filaments appeared to be associated with ribosomes and polysomes. The ultrastructural location of the GFAP mRNA (especially along the intermediate filaments) may be unique to this mRNA or may represent a more generalized mRNA phenomenon.

INTRODUCTION

Cytoplasmic intermediate filaments are a major constituent of the cytoskeleton and have been identified in almost all eucaryotic cells (for reviews, see Lazarides, 1982; Traub, 1985; Steinert and Roop, 1988; Goldman *et al.*, 1990). Although they have significant similarities, there is sufficient variation (e.g., intron and exon arrangement, primary amino acid sequence) among the different kinds of intermediate filaments to categorize them into subtypes: (I) acidic keratins; (II) neutral and basic keratins; (III) glial fibrillary acidic protein (GFAP), vimentin, desmin, and peripherin; and (IV) neurofilaments. In addition, intermediate filaments in the nucleus constitute a fifth subtype: the nuclear lamins. A potential sixth subtype, nestin, that is expressed in neuroepithelial stem cells has recently been identified (Lendahl *et al.*, 1990).

Cytoplasmic intermediate filaments are believed to be anchored to the nuclear envelope, surround the nuclear pores, extend outward throughout the cell where they interact with numerous organelles, and eventually terminate at the plasma membrane (Goldman *et al.*, 1985; Traub, 1985; Tokuyasu *et al.*, 1985; Georgatos and Blobel, 1987a,b; Georgatos *et al.*, 1987; Goldman *et al.*, 1990; Zorn *et al.*, 1990; Djabali *et al.*, 1991; Jiao *et al.*, 1991). Although the precise function(s) of the intermediate filaments is not known, structural evidence has led to the proposal that they may act as a scaffold to maintain the position of the nucleus and other organelles. Because of their strategic location surrounding the nuclear pore, it has also been proposed that intermediate filaments may act as guides or "tracks" for the transit of molecules through the pores (Goldman *et al.*, 1985).

In normal retinal Müller cells, GFAP intermediate filaments do not extend throughout the entire cell (Bignami and Dahl, 1979; O'Dowd and Eng, 1979; Dixon and Eng, 1981; Ohira *et al.*, 1984; Bjorklund *et al.*, 1985; Kivela *et al.*, 1986; Erickson *et al.*, 1987b; Vaughan *et al.*, 1990) but have a restricted distribution between the nucleus and the vitreous cavity. However, during retinal degenerations (Bignami and Dahl, 1979; Miller and Oberdorfer, 1981; Shaw and Weber, 1983; Eisenfeld *et al.*, 1984; Okada *et al.*, 1988; Sarthy and Fu, 1989a; Sarthy *et al.*, 1989b) or after retinal detachment (a separation of the retina from the adjacent retinal pigmented epithelium), GFAP intermediate filaments form an extensive network throughout the Müller cell cytoplasm (Erickson *et al.*, 1983, 1987b). This response of the Müller cells thus seems to be characteristic of inherited and acquired retinal degenerations. While the function of these intermediate filaments is not known, they do form the major cytoskeletal compo-

1047-8477/92 $3.00

nent of the subsequent Müller cell scar (Erickson *et al.*, 1983, 1987; Lewis *et al.*, 1989). This scar is analogous to other CNS astrocytic scars (Kerns and Hinsman, 1973; Kao and Chang, 1977; Kao, 1980). The Müller cell scar can block the reapposition of a detached retina to the retinal pigment epithelium following retinal reattachment surgery (Anderson *et al.*, 1986). As elsewhere in the CNS, the neurons (in this case the photoreceptors) impinging on the scar are compromised structurally and presumably functionally.

Understanding the structural and molecular events preceeding scar formation may reveal key mechanisms influencing their establishment. This study focuses upon the early increase in GFAP filament accumulation in the Müller cells, and addresses whether there is an increase in GFAP mRNA in detached retinas, and if so, whether this increase is in the astrocytes or Müller cells (or both). In addition, the ultrastructural location of GFAP mRNA is addressed to reveal any potential changes within the astrocytes and Müller cells. Preliminary reports of this study have been presented in abstract form (Erickson *et al.*, 1989b, 1990b).

MATERIALS AND METHODS

Animals. Cats (n = 9) were maintained on a 12:12 (Light: Dark) cycle for at least 2 weeks prior to euthanasia 4 hr into the light cycle. Three cat retinas were experimentally detached from the retinal pigmented epithelium (RPE) 3 days prior to euthanasia in order to stimulate GFAP expression in the retinal Müller cells (Erickson *et al.*, 1987b). Detailed methods have been published previously (Anderson *et al.*, 1986). Briefly, the lens and vitreous were removed and a 0.25% aqueous solution of Healon (sodium hyaluronate; Pharmacia) was slowly injected (using a micropipet) into the extracellular space between the photoreceptors and RPE. The resulting retinal detachment radiated outward from the retinal hole produced by the micropipet.

Tissue fixation and processing. Tissue for conventional electron microscopy was processed according to our previously published protocols (Anderson *et al.*, 1983; Erickson *et al.*, 1983). Briefly, the tissue was fixed overnight in 1% formaldehyde (from paraformaldehyde) plus 1% glutaraldehyde in phosphate buffer, postfixed in 2% osmium tetroxide, dehydrated in a graded ethanol and H_2O series, and embedded in Araldite (6005). Thin tissue sections were placed on copper grids, stained with uranyl acetate and lead citrate, carbon coated, and viewed in a Philips CM10 electron microscope.

Tissue for postembedding immunogold electron microscopy was processed according to previously published protocols (Erickson *et al.*, 1987a). Briefly, the tissue was fixed for 1.0 hr with 1% formaldehyde (from paraformaldehyde) plus 1% glutaraldehyde in 0.086 *M* sodium phosphate ($NaPO_4$) buffer, pH 7.2. It was then rinsed in 0.137 *M* $NaPO_4$ buffer and dehydrated through a graded methanol (or *N,N*-dimethylformamide, DMF) series. Secondary fixation (for 1.0 hr) was with 2.0% uranyl acetate (UAc) in the 70% methanol (or 70% DMF) step. After completing the dehydration, the tissue was embedded in LR White resin (or Lowicryl K4M resin for the DMF dehydrated tissue). Alternatively, after the primary fixation, tissue from one animal was washed in 0.05 *M* Na–H–Maleate–NaOH buffer (pH 5.2) followed by a secondary fixation in 2% UAc in Maleate buffer (pH 4.75) for 2.0 hours. Two percent UAc fixation continued during the methanol dehydration (15, 30, 50, and 70% steps, 10 min each) followed by simple methanol dehydration at 85, 95, and 100% levels. All processing steps in methanol in this series were performed at 4.0°C. Tissue was then embedded in LR White resin following the protocol listed above.

Tissue for *in situ* hybridization was fixed for 1.0 hr in either 2 or 4% formaldehyde (from paraformaldehyde) in 0.086 *M* $NaPO_4$ buffer, pH 7.2. Dehydration with increasing concentrations of DMF preceded embedding in Lowicryl K4M resin. In addition, *in situ* hybridization was attempted on the LR White-embedded tissue that was used for immunogold electron microscopy.

Immunogold electron microscopy. For the immunogold electron microscopy, we followed our previously published protocol (Erickson *et al.*, 1987a). Briefly, thin sections were placed on formvar-coated nickel grids and floated on diluted normal goat serum. After this blocking step, the grids were incubated on drops of polyclonal anti-GFAP (rabbit anti-bovine GFAP, IgG fraction, 1:400 dilution, DAKO Laboratories, Santa Barbara, CA). The sections were incubated overnight with the anti-GFAP or, for control experiments, with diluted nonimmune rabbit serum or buffer alone. After rinsing with buffer the sections were incubated on drops of secondary antibody–gold complexes (goat anti-rabbit IgG-5, -15 or -20 nm gold, 1:40 dilution, Janssen Pharmaceutica, Beerse, Belgium) for 1.0 hr. After rinsing with buffer and then ddH_2O the grids were air dried. The tissue was then stained in UAc and lead citrate followed by carbon coating and viewing in a Philips CM10 electron microscope.

SDS–PAGE and immunobloting. For the analysis of whole retina homogenates by SDS–PAGE and immunoblotting, we followed our previously published protocol (Lewis *et al.*, 1989). Briefly, cat retina was homogenized in PBS containing phenylmethylsulfonyl fluoride, EDTA, Triton X-100, and SDS to inhibit protein degradation. Protein concentrations were determined by BCA Protein Assay (Pierce Chemical Co.). Samples containing 50 μg protein were analyzed by SDS–PAGE on a 7.5–20% gradient gel. Proteins of known molecular weights (Bio-Rad) were run as standards. After separation, the proteins were stained with Coomassie blue or transferred by electroblotting to nitrocellulose membrane. After blocking with BSA (0.5%) in Tris-buffered saline (TBS, 0.02 *M* Trizma base, 0.50 *M* NaCl, pH 7.5, with concentrated HCl) the nitrocellulose membrane was incubated overnight with rabbit anti-bovine GFAP (DAKO) diluted 1:100 in TBS. After rinsing, the blot was incubated with HRP-labeled goat anti-rabbit IgG (Bio-Rad; 1:2000 in TBS) for 1.0 hr. The blot was rinsed and incubated with HRP color development reagent (Bio-Rad) for 15 min, rinsed with ddH_2O, and air-dried.

Preparation of biotinylated cDNA-encoding GFAP. A cDNA-encoding GFAP (clone G1) was generously provided by S. Lewis and N. Cowan (Lewis *et al.*, 1984). A 1.1-kb *Hin*dIII fragment was isolated by agarose gel electrophoresis. A biotinylated probe was prepared using the random primer method of Feinberg and Vogelstein (1983, 1984) using a Random Primed DNA Labeling Kit (Boehringer-Mannheim). This method yields probes of an average length of 80–120 base pairs representing sequences along the entire length of the starting cDNA. The subsequent biotinylated GFAP cDNA probe (bio-GFAP-cDNA) was purified using a 0.5-ml Sephadex G-50 column. The DNA concentration of the probe was assayed using the ethidium bromide/plastic wrap method (Maniatis *et al.*, 1982). The level of biotinylation of the bio-GFAP-cDNA was assayed using a nonradioactive nucleic acid detection system (BluGENE, Bethesda Research Laboratories). Two picograms of the bio-GFAP-cDNA were detected with this dot blot assay.

RNA gels and Northern blots. RNA was isolated according to the method of Chirgwin and colleagues (1979). Briefly, normal and 3-day detached cat retinas were frozen, homogenized in guanidinium isothiocyanate, and ultracentrifuged through cesium chloride. The RNA pellet was then resuspended and quantified by spectrophotometry. Thirty micrograms of total RNA from each sample was then fractionated using formaldehyde–

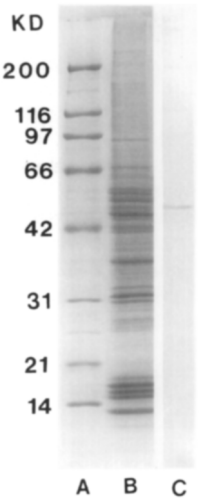

FIG. 1. Coomassie blue-stained SDS–PAGE gel of molecular weight standards (lane A) and proteins of cat retina homogenate (lane B). Lane C is an immunoblot of cat retina homogenate that was probed with the polyclonal anti-GFAP. The single band at 51 kDa (the appropriate size for GFAP) shows the specificity of the antibodies used for the immunoelectron microscopy.

agarose gel electrophoresis (Maniatis *et al.*, 1982), transferred to nitrocellulose, and probed with a GFAP-cDNA (Lewis *et al.*, 1984) that was ^{32}P-labeled by the random primer method (Feinberg and Vogelstein, 1983, 1984). As controls for the specificity of the GFAP probe, total RNA from mouse brain (positive control) and PC 12 cells (negative control) were included on the blot. As a control for loading levels, the blots were stripped and reprobed with a β tubulin-cDNA (Cleveland *et al.*, 1980).

Electron microscopic in situ hybridization. For the electron microscopic *in situ* hybridization, we combined two previously published protocols (Binder *et al.*, 1986; Wolber and Beals, 1989). Thin sections of the Lowicryl K4M- or LR White-embedded tissue were placed on nickel grids. The grids were submerged in hybridization buffer (50% formamide; 5× Denhardt's = 0.10% Ficoll, 0.10% polyvinylpyrrolidone, and 0.10% BSA; 5× SSPE = 0.75 *M* NaCl, 50 m*M* NaH_2PO_4, and 5 m*M* EDTA; 0.1% SDS; 100 μg/ml salmon sperm DNA), in the absence or presence of bio-GFAP-cDNA (0.16 ng/μl) that had been heated to 95°C for 10 min. The incubation continued overnight in a humidified chamber maintained at 37°C. After rinsing in 2× SSC (0.30 *M* NaCl and 0.030 *M* sodium citrate) at room temperature, grids were submerged in streptavidin–gold (15 nm diameter) conjugate (SA-AU, Janssen Pharmaceutica) at a 1:10 dilution in 2× SSC + 1% BSA (alternatively diluted in 20 m*M* TBS + 1% BSA). Grids remained in the SA-AU solution for 1 hr at room temperature and were subsequently rinsed in 2× SSC and fixed with 1% glutaraldehyde in 2× SSC for 30 min. After a final rinse in 2× SSC, grids were rinsed briefly in ddH_2O and allowed to air dry. The sections on the grids were subsequently stained with UAc, lead citrate, and carbon coated prior to viewing in a Philips CM10 electron microscope.

This combination of techniques yields low labeling levels due to the following: (1) the signal is not amplified using SA-AU (versus indirect immunogold detection of the bio-cDNA); (2) only mRNA on the surface of the tissue section is accessible to the bio-cDNA; and (3) the GFAP mRNA is regionally located (Sarthy *et al.*, 1989b). However, this combination of techniques yields extremely high resolution localization of the mRNA because the SA-AU is not separated from the site of hybridization as much as with indirect immunogold detection of mRNA.

RESULTS

GFAP filament localization in retinal cells. The specificity of the polyclonal antisera directed against GFAP was initially established by immunoblotting analysis. As seen in Fig. 1, immunoblots of whole retina homogenates show a single band of the appropriate molecular weight (51 kDa) for GFAP after probing with the polyclonal anti-GFAP.

Next, we analyzed the pattern of GFAP expression in the retina by immunogold electron microscopy. All of the immunocytochemistry fixation protocols yielded similar results. The anti-GFAP labeling was detected in retinal astrocytes (Fig. 2) where it specifically labeled intermediate filaments (Fig. 3). Processes from these astrocytes were found in the nerve fiber layer of the retina adjacent to the basal lamina surrounding capillary endothelial cells (Fig. 2), adjacent to ganglion cell axons, and in the optic nerve region. Ganglion cell axons and capillary endothelial cells contain numerous 10-nm-diameter

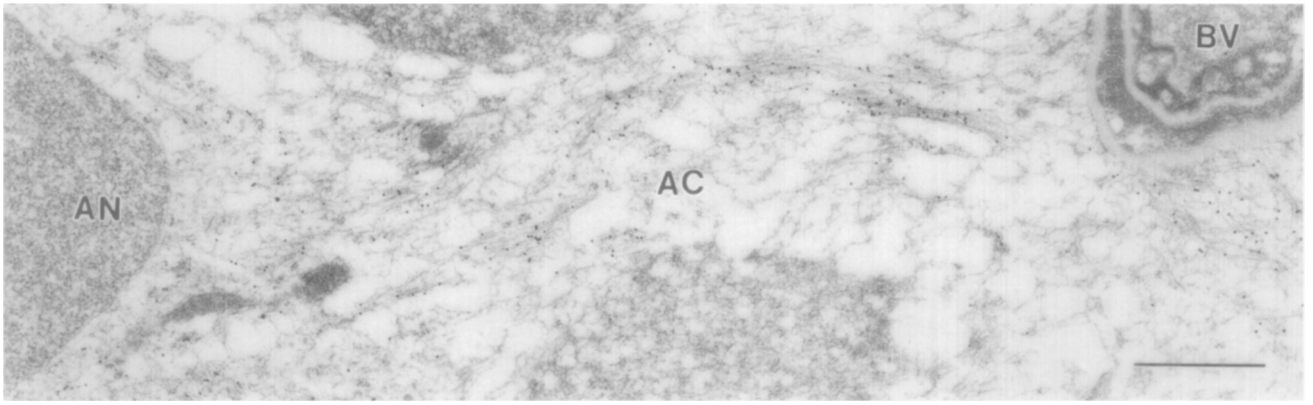

FIG. 2. Cells within the retina and optic nerve head that contained GFAP were identified by postembedding, immunogold electron microscopy. This is an example of a retinal astrocyte labeled with anti-GFAP. The astrocyte cytoplasm (AC) contains numerous intermediate filaments, labeled with anti-GFAP, between the nucleus (AN) and the plasma membrane adjacent to a retinal blood vessel (BV). Bar = 1.0 μm.

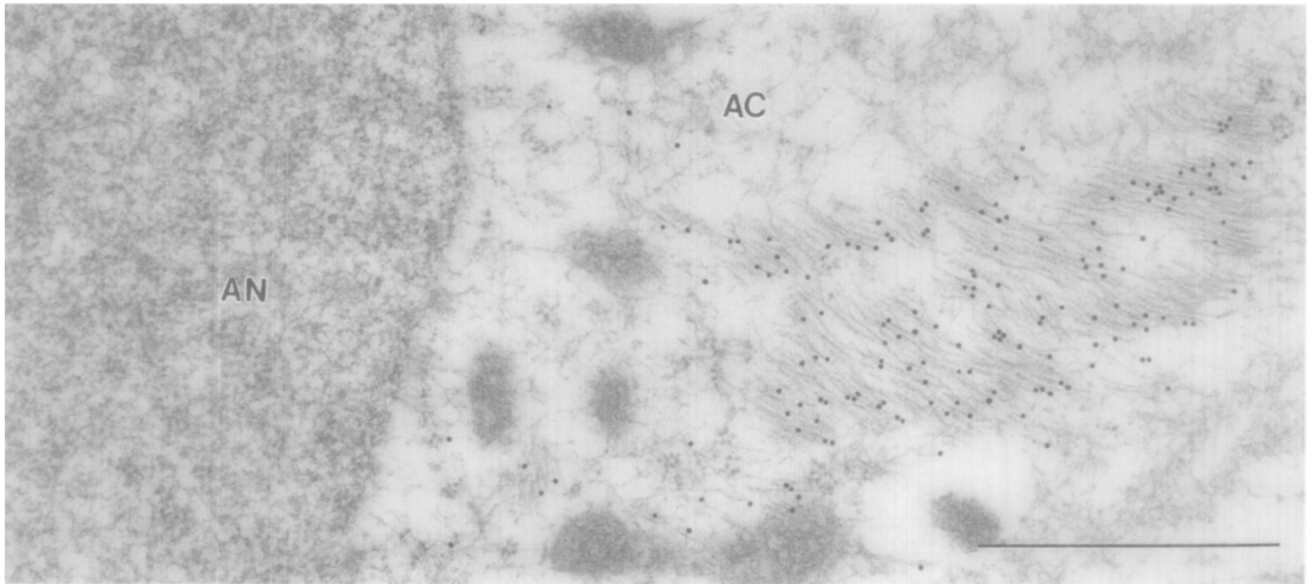

FIG. 3. At higher magnification, the anti-GFAP labeling (15-nm gold spheres) within the astrocyte cytoplasm (AC) is detected over the 10-nm-diameter intermediate filaments. Astrocyte nucleus, AN; bar = 1.0 μm.

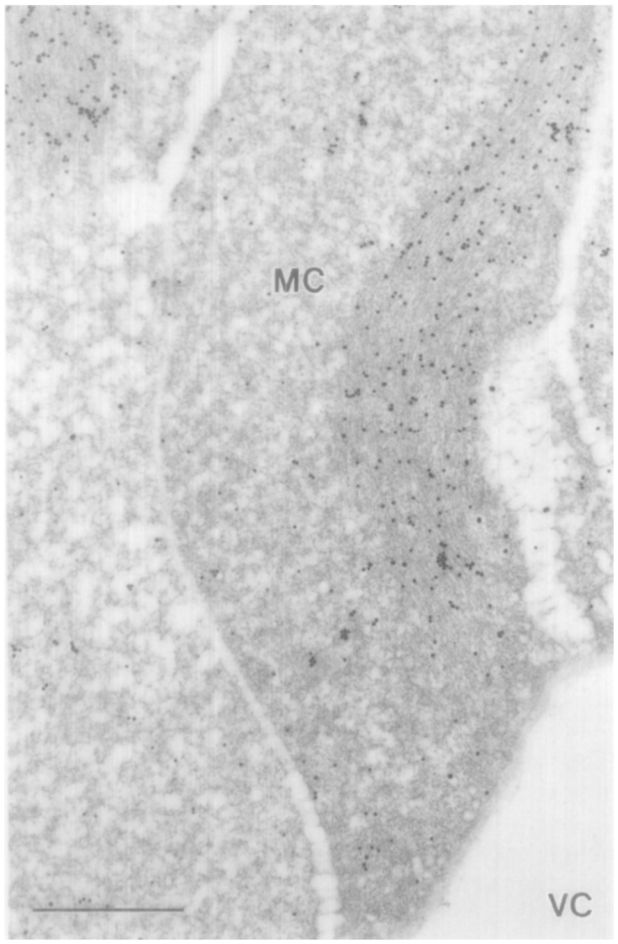

FIG. 4. The only other cells to immunolabel with the anti-GFAP were the retinal Müller cells. This is an example of labeling over the intermediate filaments of a Müller cell (MC) near the vitreous cavity (VC) from a normal retina. The anti-GFAP labeling within these cells was restricted to this inner retinal region near the vitreous cavity. Bar = 1.0 μm.

filaments but were not labeled. The only other cell type that labeled with anti-GFAP was the retinal Müller cell. The labeling in Müller cells in normal retinas occurred only near the vitreous cavity (the "end foot" region; Fig. 4). Although the gold spheres were predominantly over the 10-nm-diameter intermediate filaments, a low level of labeling was also detected over the cytoplasm in regions free of filaments. Only the cells that had labeled 10-nm-diameter filaments showed diffuse cytoplasmic labeling. All other cell types were negative for anti-GFAP labeling.

In retinas detached for 3 days, the number of 10-nm-diameter filaments within the Müller cells was elevated relative to the normal Müller cells. In addition, the cytoplasmic location and immunolabeling of the filaments extended from the end foot region of the cells, through numerous layers of the retina, into the outer nuclear layer (Fig. 5). On the other hand, there was no apparent change in the quantity or location of GFAP intermediate filaments in the retina or optic nerve astrocytes. The immunocytochemistry control tissue was unlabeled (Fig. 6).

Tissue processed for immunocytochemistry and conventional electron microscopy was analyzed for possible associations between intermediate filaments and other organelles such as the nuclear envelope, nuclear pores, ribosomes, and polysomes. Astrocytes within optic nerve, normal retina, and detached retina as well as Müller cells within detached retina revealed common intermediate filament association with ribosomes and polysomes (Fig. 7). In appropriate planes of section, intermediate filaments also appeared to associate with the nuclear

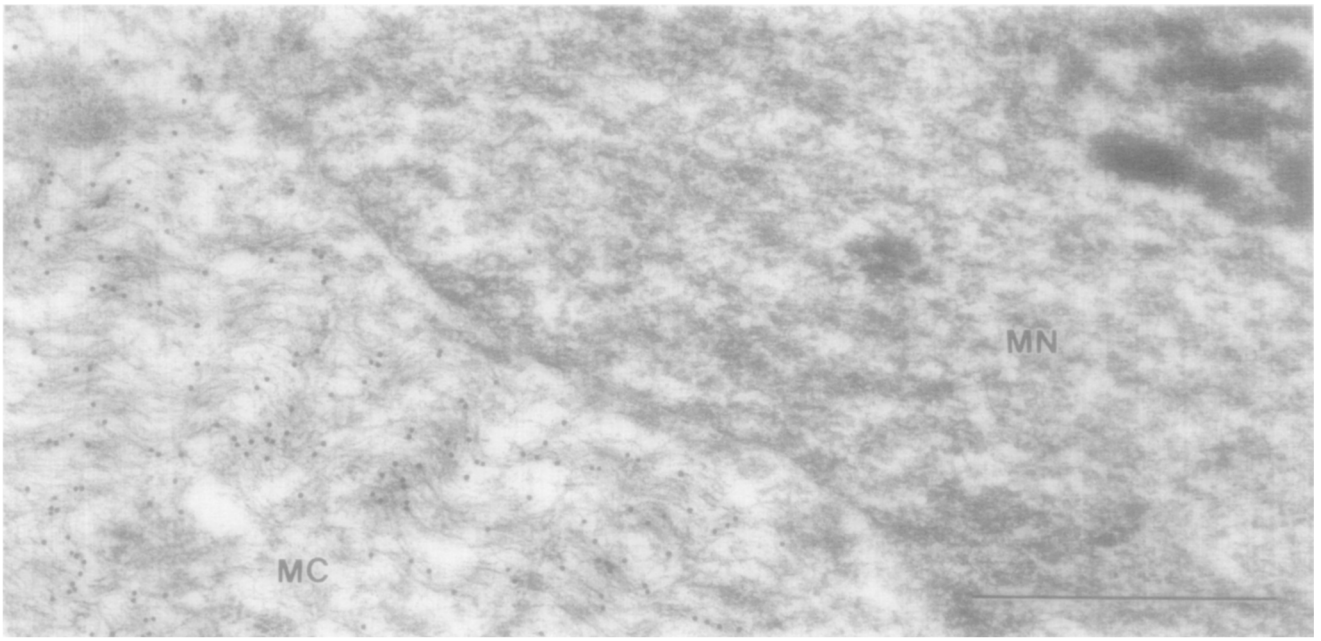

FIG. 5. Immunogold electron micrograph of a Müller cell nucleus (MN) and cytoplasm (MC) within a 3-day detached retina. This nucleus had translocated to the outer nuclear layer (they normally reside in the inner nuclear layer). The anti-GFAP labeling (15-nm gold spheres) is over the 10-nm-diameter intermediate filaments. Nuclei and labeled intermediate filaments were never detected in this region of Müller cells within normal retinas. Bar = 1.0 μm.

envelope and presumed nuclear pores (Figs. 3 and 8).

GFAP mRNA levels and ultrastructural localization. When total RNA isolated from normal and 3-day detached retinas was probed with the cDNA-GFAP (Fig. 9A), there was an approximately 500% increase in GFAP mRNA in the detached retina sample (determined by scanning densitometry). As a control for determining equal RNA loading levels, the blots were stripped and reprobed with a β tubulin cDNA (Fig. 9B). The β tubulin mRNA showed an approximately 100% increase in the detached sample.

Initial electron microscopic *in situ* hybridization experiments employing LR White-embedded tissue were plagued with high background (gold spheres located over regions of pure resin). However, using Lowicryl K4M-embedded tissue, background labeling occurred at extremely low levels (approximately 1 gold sphere per 16 μm^2, as determined by counting gold spheres per square micron in randomly selected cells and over pure resin). As a result, the data presented here is from the tissue embedded in Lowicryl K4M. In cell types that do not contain GFAP, gold spheres occurred at the same low background levels as over regions of the resin without tissue (Fig. 10).

Astrocytes in optic nerve, in normal retina, and in retina that had been detached for 3 days were clearly labeled with gold spheres representing GFAP mRNA (Fig. 11A). The labeling density in these cells occurred from a low of background levels in some regions up to approximately 10 times the background levels in other cellular regions (however, due to the regional location of labeling and the low labeling levels inherent with this technique, rigorous quantitation was not undertaken). In the nuclei, the gold spheres were most frequently located over amorphous, electron-dense regions within the euchromatin (Figs. 11B and 11C). In the cytoplasm, the label was routinely associated with the 10-nm-diameter intermediate filaments (Fig. 12). In fortu-

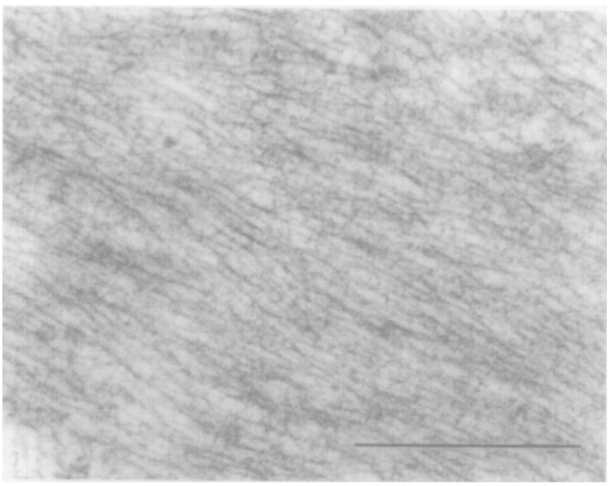

FIG. 6. Immunogold electron micrograph of a control experiment. The anti-GFAP was omitted and nonimmune rabbit serum was used as the primary antibody. No labeling was observed, even over regions of dense intermediate filaments in astrocytes or Müller cells within 3-day detached retinas (this example). Bar = 0.5 μm.

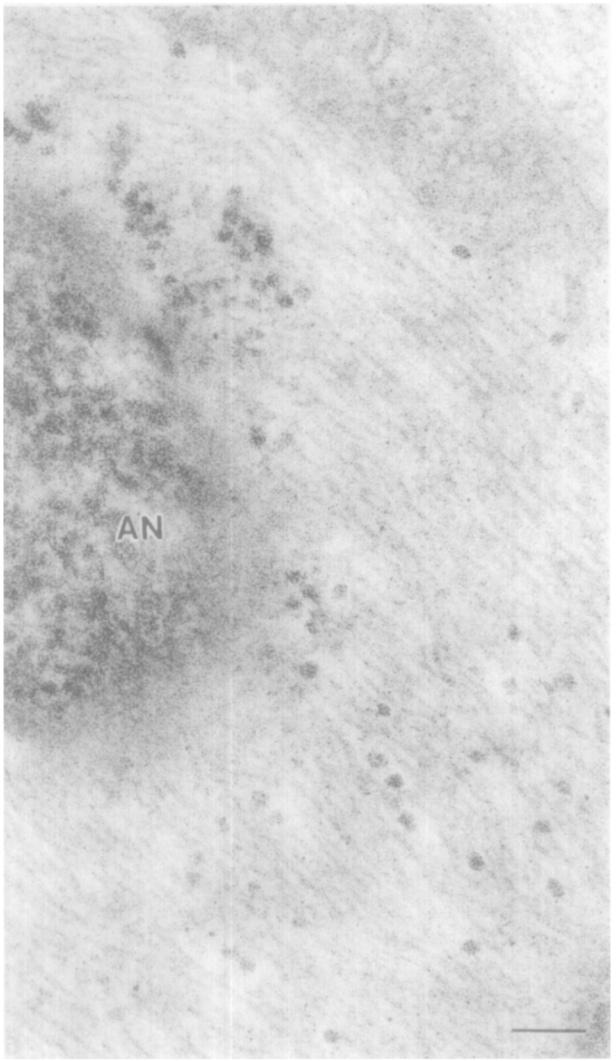

FIG. 7. Electron micrograph of an astrocyte nucleus (AN) and adjacent cytoplasm from normal retina that was processed for conventional electron microscopy. Numerous ribosomes and polysomes can be seen associating with the intermediate filaments. Bar = 0.1 μm.

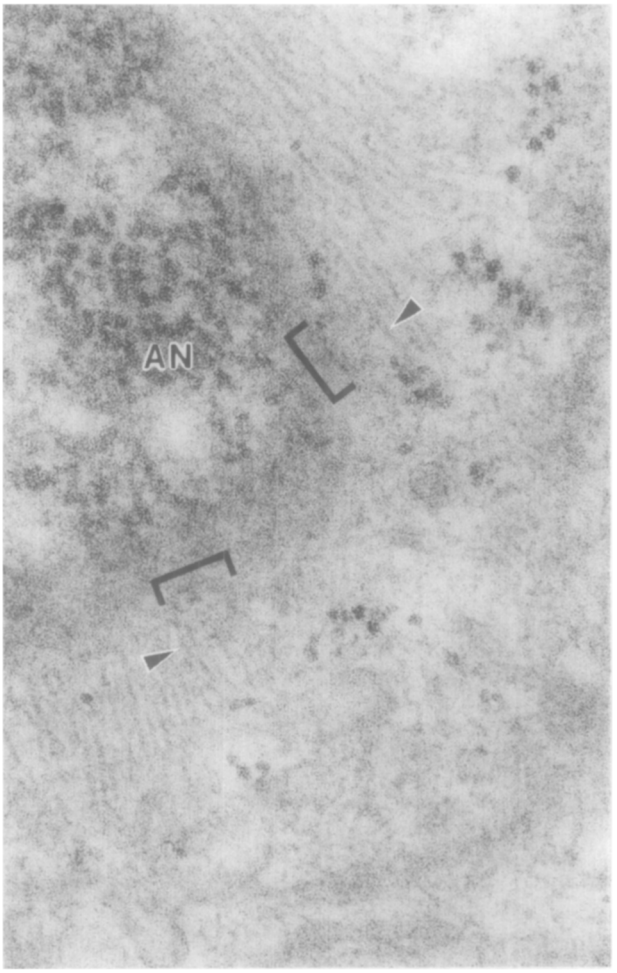

FIG. 8. Electron micrograph of an astrocyte nucleus (AN) and adjacent cytoplasm from normal retina that was processed for conventional electron microscopy. *En face* views of nuclear envelope and presumed nuclear pores (brackets) suggest intimate associations between these structures and intermediate filaments. Two filaments are indicated by arrowheads. Bar = 0.1 μm.

itous tissue sections, that resulted in *en face* views of the presumed nuclear pores, intermediate filaments labeled with gold spheres sometimes appeared to be associating with the pores (Fig. 13). Figure 14 shows a polysomal cluster and gold spheres associating with intermediate filaments. Ribosomes and polysomes, located along intermediate filaments, were routinely labeled in these cells (Fig. 15). Rarely, gold spheres could also be found associated with intermediate filaments near segments of rough endoplasmic reticulum (Fig. 16).

Gold spheres above background levels were not detected in Müller cells from normal retinas with this technique (data not shown), where expression of GFAP is very low. However, in Müller cells from 3-day detached retinas, labeling was observed over the same structures and in the same density range as in optic nerve and retinal astrocytes. In the nuclei, gold was most frequently observed in amorphous, electron-dense regions within the euchromatin (Fig. 17). Labeling over the region of the Müller cells between the nucleus and the outer limiting membrane was infrequent compared to the region between the nucleus and the vitreous cavity (Fig. 18). The labeling pattern in this "inner" region of the cytoplasm was identical to that found in astrocytes, i.e., associated with intermediate filaments, ribosomes and polysomes. We did not detect any labeling associated with other components of the cytoskeleton, such as microtubules or microfilaments.

DISCUSSION

There is an increase in GFAP- and vimentin-containing intermediate filaments within Müller cells in 30- and 60-day detached retinas, as determined by protein gels, immunoblotting analysis,

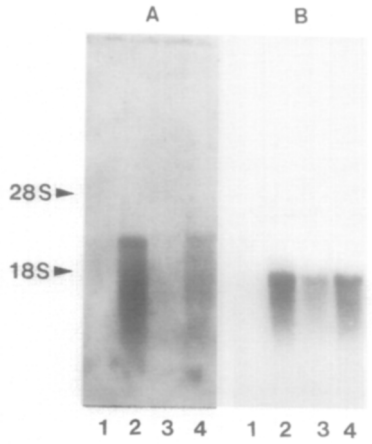

FIG. 9. Total RNA from PC12 cells (lane 1), mouse brain (lane 2), normal cat retina (lane 3), and 3-day detached cat retina (lane 4) was fractionated and transferred to nitrocellulose. The RNA blot was probed with ^{32}P-labeled GFAP cDNA (A), stripped, and reprobed with ^{32}P-labeled β tubulin cDNA (B). Panel A required 14 days for the film to reveal the GFAP mRNA in normal cat retina at sufficient levels to be read by laser scanning densitometry (which detected a 500% increase in the detached retina sample). Mouse brain GFAP mRNA (the GFAP cDNA homologue) showed the specificity of the probe, whereas the PC12 cells were negative (they contain no GFAP mRNA). Panel B required only 1 day for the film to reveal the β tubulin mRNA at sufficient levels for densitometric comparison (which detected a 100% difference between normal and detached retinas). PC12 cells have β tubulin mRNA but it is not revealed at this short exposure time.

and light- and electron-microscopic immunocytochemistry (Erickson *et al.*, 1987b; Lewis *et al.*, 1989). As determined by tissue autoradiography, there is an increase in [^{3}H]uridine incorporation within

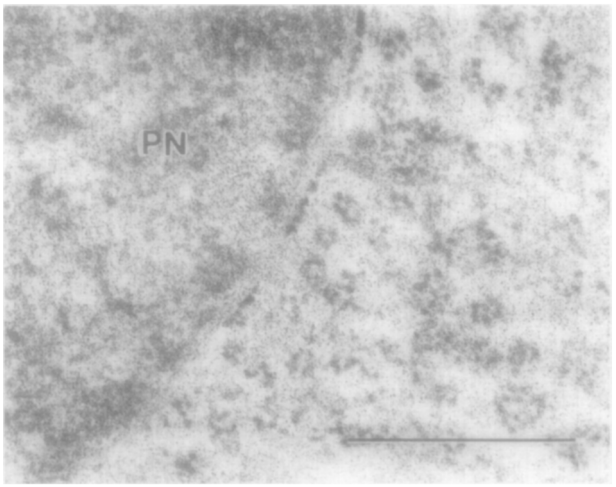

FIG. 10. Electron micrograph of a photoreceptor nucleus (PN) and cytoplasm within a 3-day detached retina. This tissue was processed for postembedding electron microscopic *in situ* hybridization (EMISH). Tissue sections were labeled with biotinylated GFAP cDNA followed by streptavidin–gold (15 nm diameter) conjugate. This cell is void of gold spheres, but is nearby the labeled Müller cell seen in Fig. 17. Photoreceptors, and each of the other cell types without GFAP, were labeled at background levels of 1 gold sphere per 16 μm^2 (approximately 2 gold spheres per cell). Bar = 0.5 μm.

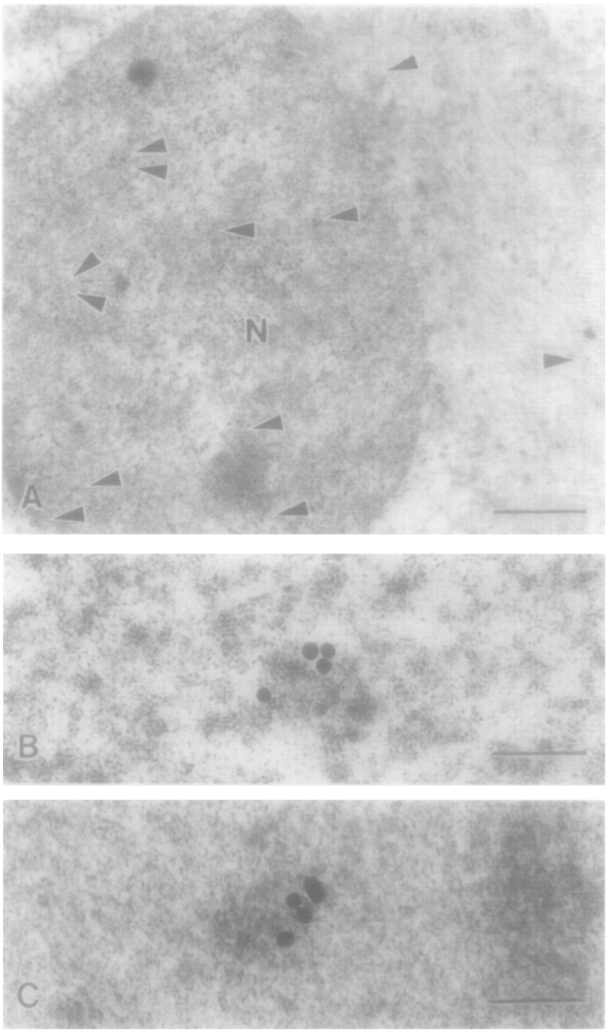

FIG. 11. Electron micrographs of EMISH-processed tissue showing an astrocyte within a retina detached for 3 days. At low magnification (A, bar = 1.0 μm), the gold spheres (indicated by arrowheads) can be seen over regions of the euchromatin within the nucleus (AN) and in the cytoplasm. At high magnification (B and C, bars = 0.1 μm), the gold spheres within the nucleus are located over amorphous, electron-dense regions within the euchromatin.

Müller cells between 2 and 3 days after retinal detachment which suggests that an increase in RNA synthesis may occur at that time (Erickson and Fisher, 1990; Erickson *et al.*, 1990a). The RNA blotting analysis and *in situ* hybridization data from this study suggests that GFAP mRNA is among the species of RNA induced (approximately fivefold) between 2 and 3 days after detachment (we have not yet addressed the issue of vimentin mRNA). Studies by Sarthy and Fu (1989a) showed an 8- to 10-fold increase in GFAP mRNA from mice retinas with an inherited retinal degeneration and a 15- to 20-fold increase after 2 weeks of light damage. In each of these examples, this appears to be active GFAP mRNA in that more GFAP-containing intermediate

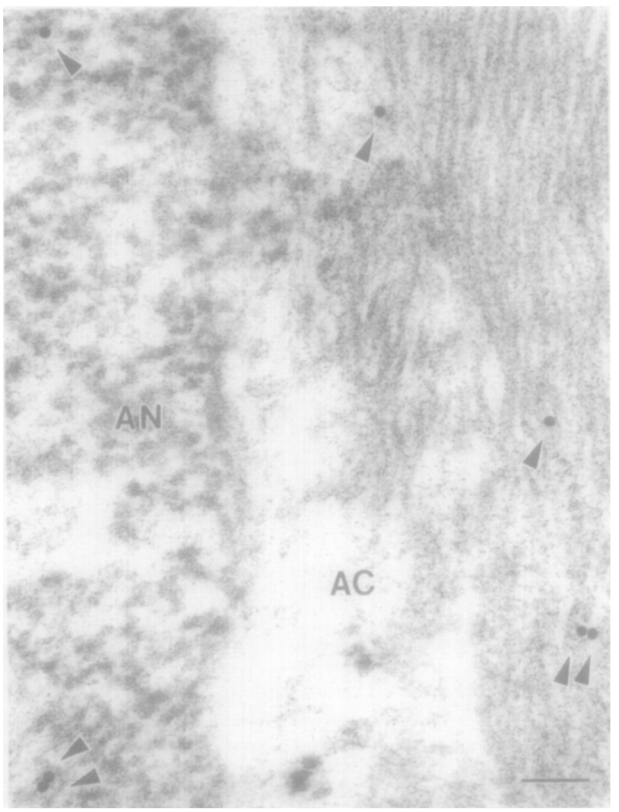

FIG. 12. High magnification view of EMISH-processed tissue showing the edge of the nucleus (AN) and adjacent cytoplasm from an optic nerve astrocyte. The gold spheres in the nucleus are located over amorphous, electron-dense regions within the euchromatin. In the cytoplasm, gold spheres (15 nm diameter) are routinely found associated with 10-nm diameter intermediate filaments. Bar = 0.1 μm.

filaments are present in the cells (as determined in the present case by immunoelectron microscopy; our preliminary unpublished data suggests that vimentin is also a component of these intermediate filaments).

An increase in GFAP appears to be a general feature in other CNS areas during reactive gliosis whether the primary injury is due to trauma, infection, a metabolic defect, or an autoimmune response (for review see Eng, 1988). Studies aimed at revealing potential control of GFAP levels have shown the importance of growth factors and hormones in stimulating an increase in GFAP accumulation in astrocytes in culture (Morrison *et al.*, 1985; Perraud *et al.*, 1988). One of these, basic fibroblast growth factor (bFGF), has been shown by recent studies to be present within the interphotoreceptor matrix (IPM) between the photoreceptors and the adjacent retinal pigment epithelium (Hageman *et al.*, 1991). It is this area that is disrupted during retinal detachment. The potential release of bFGF from the disrupted IPM could stimulate the Müller cells, which have microvilli that protrude into the IPM.

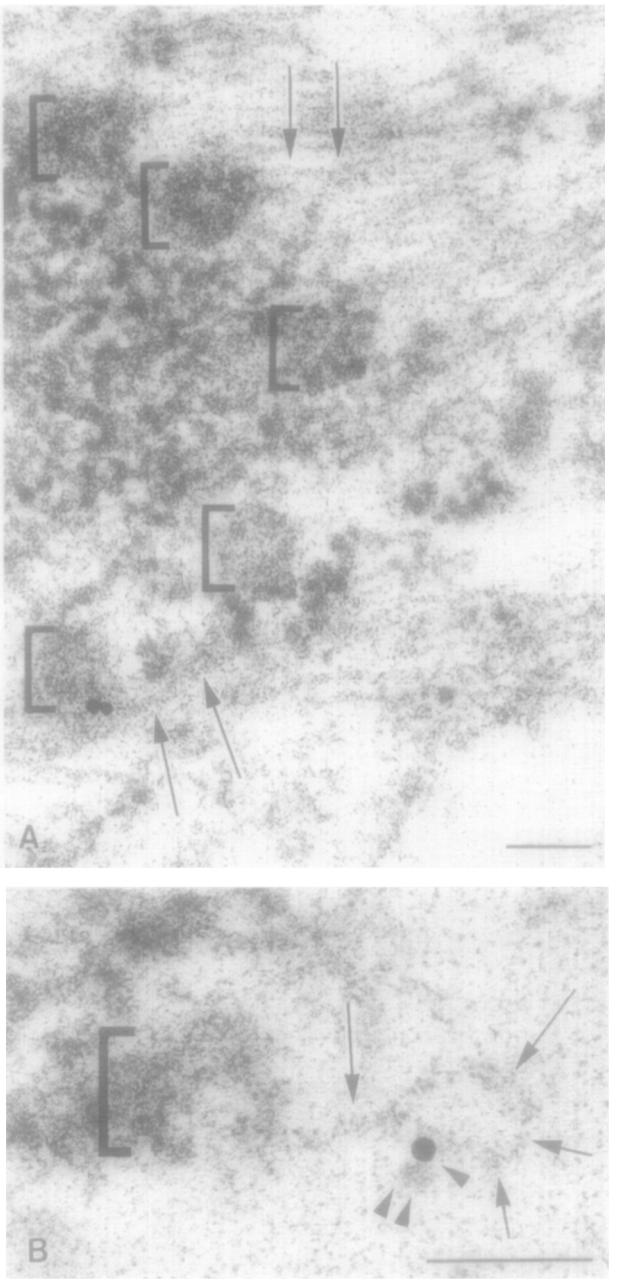

FIG. 13. The edge of a nucleus, cut *en face*, showing presumed nuclear pores (brackets) and the adjacent cytoplasm from an astrocyte in the optic nerve (EMISH-processed tissue). In fortuitous sections (A), gold spheres (arrowheads) can be found adjacent to the presumed nuclear pore along intermediate filaments (arrows) which appear to associate with the periphery of the pores. In B, a gold sphere (single arrowhead) is located between an intermediate filament (arrows), where it leaves the plane of this section, and a presumed ribosome (double arrowheads). Bars = 0.1 μm.

Whether bFGF, hormones, or other molecules induce GFAP mRNA, the resulting GFAP filament network is the major cytoskeletal outcome. It has been suggested that intermediate filaments provide a cytoskeletal framework upon which organelles and molecules may be organized (Lazarides, 1982; Goldman *et al.*, 1985, 1990). Intermediate filaments

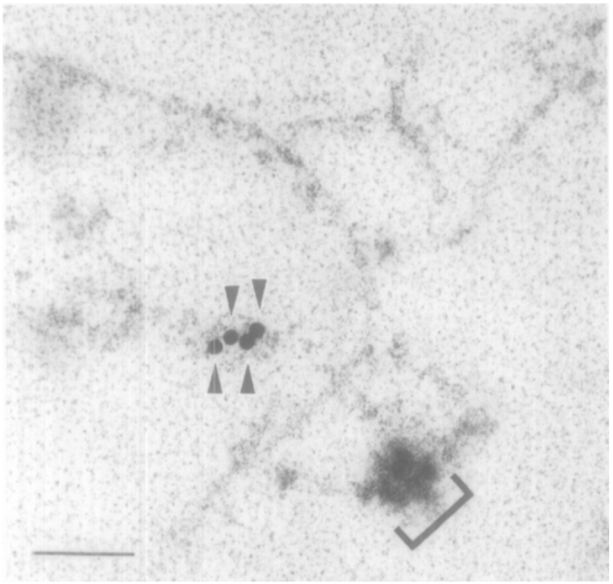

FIG. 14. A polysomal cluster (bracket), associated with intermediate filaments, and nearby gold spheres (arrowheads) within an astrocyte (EMISH-processed tissue). Bar = 0.1 μm.

appear to originate from the nuclear envelope, especially around the nuclear pores, extend into the cytoplasm where they associate with various organelles (i.e., polysomes, vesicles, mitochondria), and terminate at the plasma membrane (Goldman *et al.*, 1985; Traub, 1985; Tokuyasu *et al.*, 1985; Georgatos and Blobel, 1987a,b; Georgatos *et al.*, 1987; Goldman *et al.*, 1990; Zorn *et al.*, 1990; Djabali *et al.*, 1991; Jiao *et al.*, 1991). Goldman and his colleagues (1985) suggested that in addition to serving as a cytoskeletal framework, intermediate filaments may function as tracks for the movement of molecules and macromolecular complexes into and out of

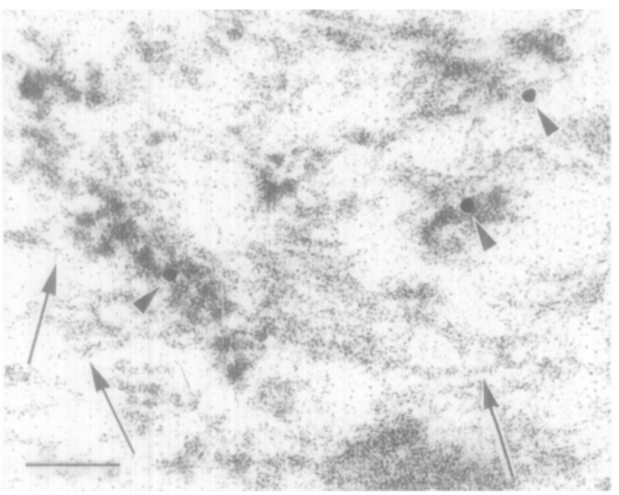

FIG. 15. In tissue processed for EMISH, intermediate filaments (arrows) are frequently found associated with labeled polysomes and ribosomes (arrowheads) within astrocytes. Bar = 0.1 μm.

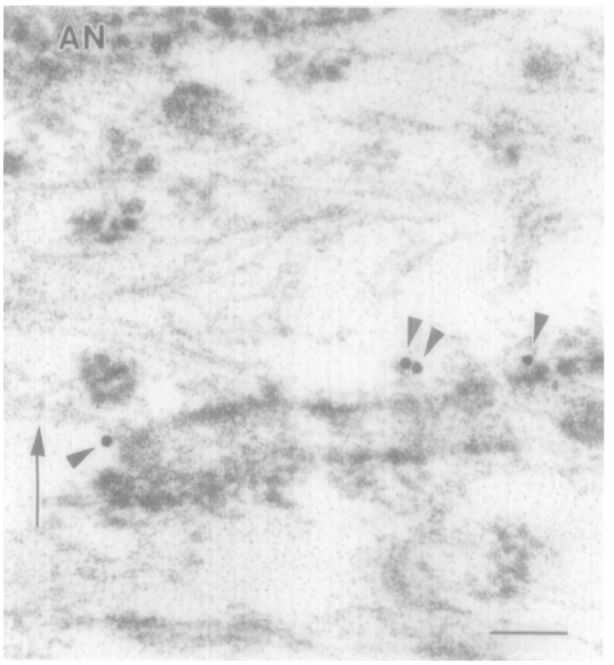

FIG. 16. Astrocyte nucleus (AN) and cytoplasm (EMISH-processed tissue). Gold spheres (arrowheads) could be found along segments of rough endoplasmic reticulum (RER). In fortuitous planes of section, gold spheres could also be found associated with intermediate filaments (arrow) that appear to also associate with RER (see the arrowhead that is near the arrow, 15-nm gold sphere, a short segment of a 10-nm intermediate filament and adjacent RER). Bar = 0.1 μm.

the nucleus. Messenger RNAs and ribosomal subunits, for example, enter the cytoplasm separately through the nuclear pores (Clawson *et al.*, 1985; Agutter, 1985b; Schumm and Webb, 1985; Schroder *et al.*, 1987, 1988; Dworetzky and Feldherr, 1988; Goldfarb and Michaud, 1991). Once they are in the cytoplasm the ribosomal subunits attach to the mRNA and translation may commence.

There is considerable evidence suggesting an association between mRNA and the cytoskeleton (Hesketh and Pryme, 1991). For example, both a structural relationship between ribosomes and the cytoskeleton (Lenk *et al.*, 1977; Wolosewick and Porter, 1979) and a functional relationship between mRNA translation and mRNA binding to a cytoskeletal framework have been observed (Cervera *et al.*, 1981; van Venrooij *et al.*, 1981). Ultrastructurally, many polyribosomes can be seen associated with the intermediate filament component of the cytoskeleton (see Figs. 2A and 2B in Lenk *et al.*, 1977; Fig. 1 in Cervera *et al.*, 1981; and this study). Additionally, disruption of microfilaments by cytochalasin B results in a biochemically detectable loss of ribosomes from the cell (Lenk *et al.*, 1977; Cervera *et al.*, 1981), suggesting some ribosomes may also be associated with actin filaments. These same studies showed that mRNA remains attached to the cytoskeleton

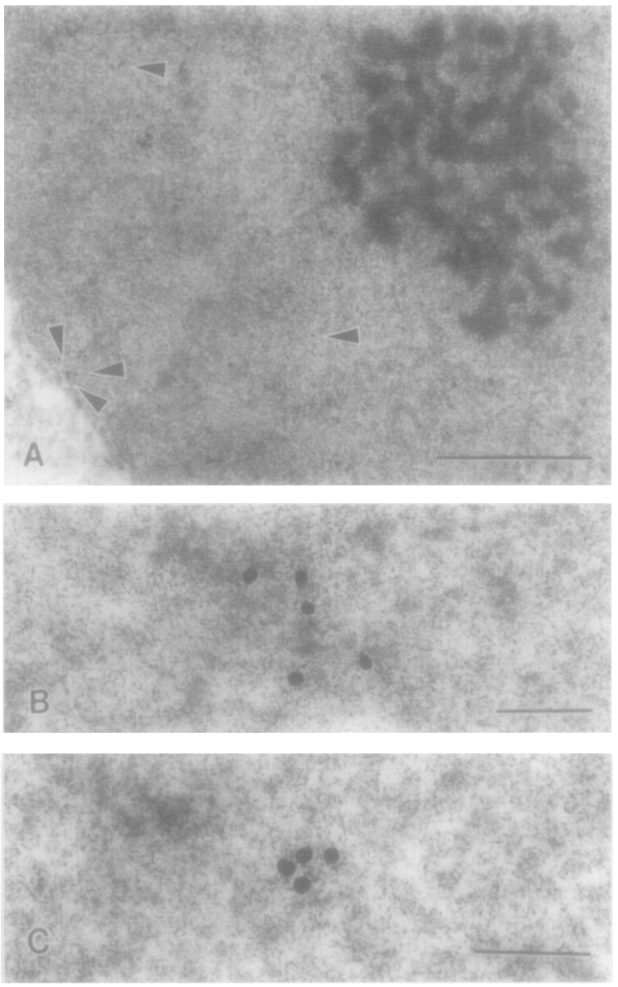

FIG. 17. Müller nucleus that had translocated into the outer nuclear layer and was found near the photoreceptor cell seen in Fig. 10 (EMISH-processed tissue). At low magnification (A, bar = 1.0 μm), the gold spheres (arrowheads) can be seen over regions within the euchromatin. At high magnification (B and C, bar = 0.1 μm), the gold spheres within the nucleus are located over amorphous, electron dense regions within the euchromatin.

even when ribosomes are removed from the cytoskeleton.

An independent route of investigation suggested a possible functional relationship between intermediate filaments and active translation (Zumbe and Trachsel, 1980; Zumbe *et al.*, 1982). Zumbe and Trachsel utilized immunofluorescence microscopy with antibodies specific for the 5′ cap structure of mRNAs (cap binding protein, CBP), and antibodies to intermediate filaments, microtubules, or actin filaments. They found the CBP (and by inference, mRNA) exhibited a cytoplasmic distribution similar to that of intermediate filaments, but not microtubules or actin filaments. Additional evidence was produced by Bachmann and colleagues (1986) when they showed by immunofluorescence that Ro protein, which appears to participate in translation-related events (Walter and Blobel, 1982), colocalizes with intermediate filaments. However, due to the limited resolution of immunofluorescence, it could not be determined if CBP or Ro were associated directly with intermediate filaments or bound to an independent structure linked to the intermediate filaments.

By light microscopic *in situ* hybridization, Lawrence and Singer (1986) detected polyadenylated RNA homogeneously distributed throughout the cell (embryonic chick skeletal myoblasts and fibroblasts in culture), vimentin mRNA near the nucleus, tubulin mRNA in the peripheral cytoplasm, and actin mRNA in lamellipodia. They suggested that ". . . localized concentrations of specific proteins may result from corresponding localization of their respective mRNAs." These results were extended in subsequent work using electron microscopic *in situ* hybridization and immunoelectron microscopy (Singer *et al.*, 1989). They suggested that the regionally distributed mRNAs for the cytoskeletal proteins were associated with actin filaments and not microtubules or intermediate filaments. How the mRNAs came to be regionally distributed remains to be determined.

In more recent studies, Sarthy and his colleagues (1989a,b) have detected GFAP mRNA in normal and degenerating mouse retinas by light microscopic *in situ* hybridization. In normal retinas, they detected GFAP mRNA only in the astrocytes, whereas in the degenerating retinas they also detected GFAP mRNA in the Müller cell cytoplasm. Within the Müller cells, the mRNA was in the region where the highest concentration of intermediate filaments occur (between the nucleus and vitreous cavity). Sarthy and his colleagues suggested that there may be an intimate relationship between GFAP mRNA and the GFAP filaments. Trimmer and colleagues (1991) have also located GFAP mRNA by light microscopic *in situ* hybridization (in astrocytes in culture) and found the mRNA located in the cell body and cellular processes where the intermediate filaments reside. Our results corroborate the data from these earlier studies regarding the regional localization of GFAP mRNA and give evidence for an intimate relationship between GFAP mRNA and the GFAP filaments. Our data also corroborates the earlier biochemical and immunofluorescence data suggesting that mRNA can be associated with intermediate filaments. In addition, our data provides evidence supporting models of potential intermediate filament function (1) as "tracks" through the nuclear pores (Goldman *et al.*, 1985) and (2) as a component of the "extended cytoskeleton" which physically links gene expression with the extracellular matrix (Bissel *et al.*, 1982). Our data might also be interpreted as preliminary structural evidence regarding GFAP

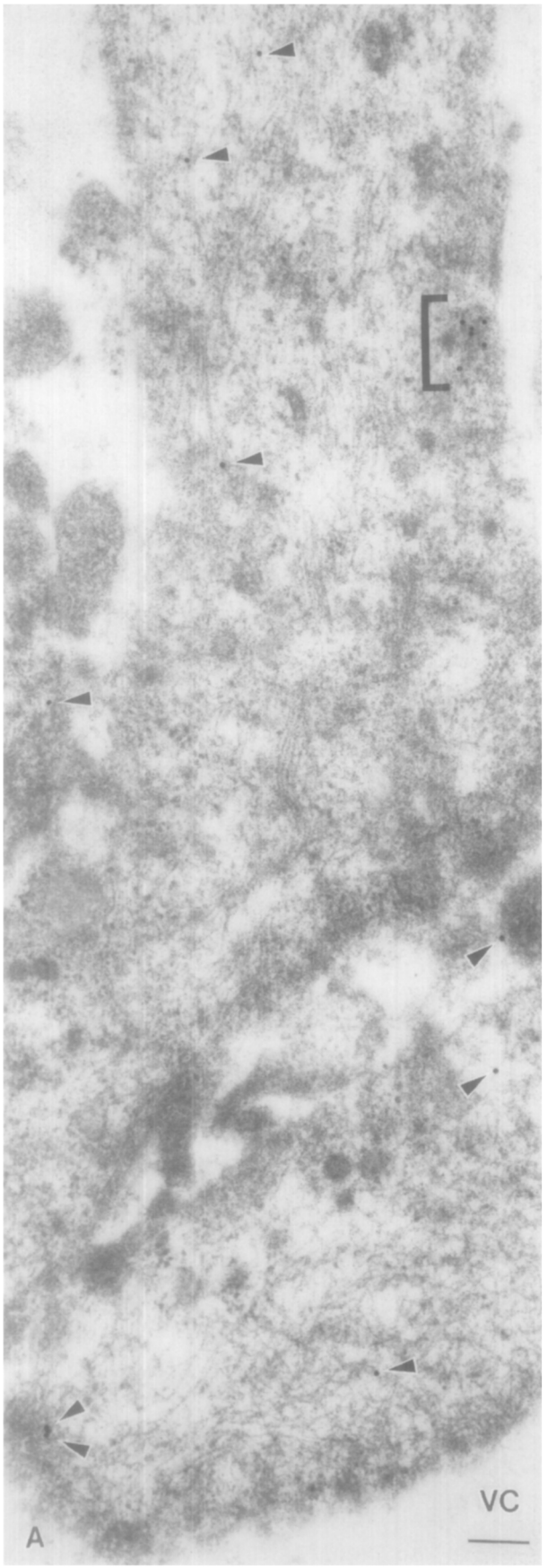

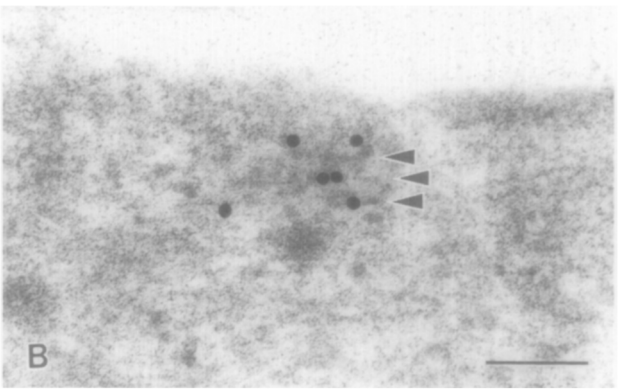

FIG. 18. Müller cell cytoplasm near the vitreous cavity (VC) in a retina detached for 3 days (EMISH-processed tissue). A is a low magnification view showing the overall labeling level in this region (gold spheres are indicated by arrowheads; the bracketed area is enlarged in B). The arrowheads in B indicate labeled intermediate filaments that are difficult to see because they come into, and go out of, the plane of this thin section. These labeled intermediate filaments are approximately 100 μm away from the nucleus. Bar = 0.1 μm.

intermediate filaments as a potential site where GFAP mRNA (and possibly other mRNA) associates with the ribosomal subunits. It should be noted that the association of GFAP mRNA with GFAP intermediate filaments may be unique to these molecules, possibly important for the translation of GFAP monomers and the assembly of the GFAP intermediate filament system. However, the current biochemical and immunofluorescent literature outlined above suggests that there appear to be other mRNAs associated with intermediate filaments. It is not yet clear why this may be occurring; however, it is possible that intermediate filaments may be involved in establishing the regional distribution of some mRNAs.

Supported by Research Grant EY-00888 (S.K.F.) from the National Eye Institute, National Institute of Health, and by the U.C.S.B. Academic Senate (S.C.F., S.K.F.).

REFERENCES

Agutter, P. S. (1985a) RNA processing, RNA transport and nuclear structure. *UCLA Symp. Mol. Cell. Biol.* **26**, 539–559.

Agutter, P. S. (1985b) Nuclear envelope NTPase and RNA efflux. *UCLA Symp. Mol. Cell. Biol.* **26**, 561–578.

Amit, A. G., Marivzza, R. A., Phillips, S. E., and Poljak, R. J. (1986) Three-dimensional structure of an antigen–antibody complex at 2.8 A. *Science* **233**, 747–753.

Anderson, D. H., Stern, W. H., Fisher, S. K., Erickson, P. A., and Borgula, G. A. (1983) Retinal detachment in the cat: The pigment epithelial–photoreceptor interface. *Invest. Ophthalmol. Visual Sci.* **24**, 906–926.

Anderson, D. H., Guerin, C. J., Erickson, P. A., Stern, W. H., and Fisher, S. K. (1986) Morphological recovery in the reattached retina. *Invest. Ophthalmol. Visual Sci.* **27**, 168–183.

Bachmann, M., Mayet, W. J., Schroder, H. C., Pfeifer, K., Meyer zum Buschenfelde, K.-H., and Müller, W. E. G. (1986) Associ-

ation of La and Ro antigens with intracellular structures in HEp-2 carcinoma cells. *Proc. Natl. Acad. Sci. USA* **83**, 7770–7774.

Bignami, A., and Dahl, D. (1979) The radial glia of Müller in the rat retina and their response to injury. An immunofluorescence study with antibodies to the glial fibrillary acidic (GFA) protein. *Exp. Eye Res.* **28**, 63–69.

Binder, M., Tourmente, S., Roth, J., Renaud, M., and Gehring, W. J. (1986) *In situ* hybridization at the electron microscopic level: Localization of transcripts on ultrathin sections of lowicryl K4M-embedded tissue using biotinylated probes and protein-A–gold complexes. *J. Cell Biol.* **102**, 1646–1653.

Bissell, M. J., Hall, H. G., and Parry, G. (1982) How does the extracellular matrix direct gene expression? *J. Theor. Biol.* **99**, 31–68.

Bjorklund, H., Bignami, A., and Dahl, D. (1985) Immunohistochemical demonstration of glial fibrillary acidic protein in normal rat Müller glia and astrocytes. *Neurosci. Lett.* **54**, 363–368.

Cervera, M., Dreyfuss, G., and Penman, S. (1981) Messenger RNA is translated when associated with the cytoskeletal framework in normal and VSV-infected HeLa cells. *Cell* **23**, 113–120.

Chirgwin, J. M., Przybyla, A. E., MacDonald, R. J., and Rutter, W. J. (1979) Isolation of biologically active ribonucleic acid from sources enriched in ribonuclease. *Biochemistry* **18**, 5294–5299.

Clawson, G. A., Feldherr, C. M., and Smuckler, E. A. (1985) Nucleocytoplasmic RNA transport (review). *Mol. Cell. Biochem.* **67**, 87–100.

Cleveland, D. W., Lopata, M. A., MacDonald, R. J., Cowan, N. J., Rutter, W. J., and Kirschner, M. W. (1980) Number and evolutionary conservation of alpha- and beta-tubulin and cytoplasmic beta- and gamma-actin genes using specific cloned cDNA probes. *Cell* **20**, 95–105.

Dixon, R. G., and Eng, L. F. (1981) Glial fibrillary acidic protein in the retina of the developing albino rat: An immunoperoxidase study of paraffin-embedded tissue. *J. Comp. Neurol.* **195**, 305–321.

Djabali, K., Portier, M. M., Gros, F., Blobel, G., and Georgatos, S. D. (1991) Network antibodies identify nuclear lamin B as a physiological attachment site for peripherin intermediate filaments. *Cell* **64**, 109–121.

Dworetzky, S. I., and Feldherr, C. M. (1988) Translocation of RNA-coated gold particles through the nuclear pores of oocytes. *J. Cell Biol.* **106**, 575–584.

Eisenfeld, A. J., Bunt-Milam, A. H., and Sarthy, P. V. (1984) Müller cell expression of glial fibrillary acidic protein after genetic and experimental photoreceptor degeneration in the rat retina. *Invest. Ophthalmol. Visual Sci.* **25**, 1321–1328.

Ekstrom, P., Sanyal, S., Narfstrom, K., Chader, G. J., and van Veen, T. (1988) Accumulation of glial fibrillary acidic protein in Müller radial glia during retinal degeneration. *Invest. Ophthalmol. Visual Sci.* **29**, 1363–1371.

Eng, L. F. (1988) Regulation of glial intermediate filaments in astrogliosis, *In* Norenberg, M. D., Hertz, L., and Schousboe, A., (Eds.), The Biochemical Pathology of Astrocytes, pp. 79–90. Alan R. Liss, New York.

Erickson, P. A., Fisher, S. K., Anderson, D. H., Stern, W. H., and Borgula, G. A. (1983) Retinal detachment in the cat: The outer nuclear and outer plexiform layers. *Invest. Ophthalmol. Visual Sci.* **24**, 927–942.

Erickson, P. A., Anderson, D. H., and Fisher, S. K. (1987a) Use of uranyl acetate *en bloc* to improve tissue preservation and labeling for post-embedding immunoelectron microscopy. *J. Electron Microsc. Tech.* **5**, 303–314.

Erickson, P. A., Fisher, S. K., Guerin, C. J., Anderson, D. H., and Kaska, D. D. (1987b) Glial fibrillary acidic protein increases in Müller cells after retinal detachment. *Exp. Eye Res.* **44**, 37–48.

Erickson, P. A., Feinstein, S. C., Lewis, G. P., and Fisher, S. K. (1989a) Glial fibrillary acidic protein messenger RNA increases following retinal detachment. *Invest. Ophthalmol. Visual Sci.* **30**, 207.

Erickson, P. A., Feinstein, S. C., Lewis, G. P., and Fisher, S. K. (1989b) Glial fibrillary acidic protein messenger RNA increases following retinal detachment. *Invest. Ophthalmol. Visual Sci.* **30**, 207a.

Erickson, P. A., and Fisher, S. K. (1990) Tritiated uridine labeling of the retina: Variations among retinal quadrants, and between right and left eyes. *Exp. Eye Res.* **51**, 145–152.

Erickson, P. A., Guerin, C. J., and Fisher, S. K. (1990a) Tritiated uridine labeling of the retina: Changes after retinal detachment. *Exp. Eye Res.* **51**, 153–158.

Erickson, P. A., Feinstein, S. C., Lewis, G. P., and Fisher, S. K. (1990b) Detection of mRNA-GFAP by post-embedding electron microscopic *in situ* hybridization. *Proc. 12th Intl. Congr. Electron Microsc.* **3**, 746–747a.

Feinberg, A. P., and Vogelstein, B. (1983) A technique for radiolabeling DNA restriction endonuclease fragments to high specific activity. *Anal. Biochem.* **132**, 6–13.

Feinberg, A. P., and Vogelstein, B. (1984) A technique for radiolabeling DNA restriction endonuclease fragments to high specific activity (addendum). *Anal. Biochem.* **137**, 266–267.

Fulton, A. B., Wan, K. M., and Penman, S. (1980) The spatial distribution of polyribosomes in 3T3 cells and the associated assembly of proteins into the skeletal framework. *Cell* **20**, 849–857.

Georgatos, S. D., and Blobel, G. (1987a) Two distinct attachment sites for vimentin along the plasma membrane and the nuclear envelope in avian erythrocytes: A basis for vectorial assembly of intermediate filaments. *J. Cell Biol.* **105**, 105–115.

Georgatos, S. D., and Blobel, G. (1987b) Lamin B constitutes an intermediate filament attachment site at the nuclear envelope. *J. Cell Biol.* **105**, 117–125.

Georgatos, S. D., Weber, K., Geisler, N., and Blobel, G. (1987) Binding of two desmin derivatives to the plasma membrane and the nuclear envelope of avian erythrocytes: Evidence for a conserved site-specificity in intermediate filament-membrane interactions. *Proc. Natl. Acad. Sci. USA* **84**, 6780–6784.

Goldfarb, D., and Michaud, N. (1991) Pathways for the nuclear transport of proteins and RNAs. *Trends Cell Biol.* **1**, 20–24.

Goldman, R., Goldman, A., Green, K., Jones, J., Lieska, N., and Yang, H.-Y. (1985) Intermediate filaments: Possible functions as cytoskeletal connecting links between the nucleus and the cell surface. *Ann. NY Acad. Sci.* **455**, 1–17.

Goldman, R. D., Zackroff, R. V., and Steinert, P. M. (1990) Intermediate filaments: An overview, *in* Goldman, R. D., and Steinert, P. M. (Eds.), Cellular and Molecular Biology of Intermediate Filaments, pp. 3–17, Plenum Press, New York.

Hageman, G. S., Kirchoff-Rempe, M. A., Lewis, G. P., Fisher, S. K., and Anderson, D. H. (1991) Sequestration of basic fibroblast growth factor in the primate retinal interphotoreceptor matrix. *Proc. Natl. Acad. Sci. USA* **88**, 6706–6710.

Hesketh, J. E., and Pryme, I. F. (1991) Review article: Interaction between mRNA, ribosomes and the cytoskeleton. *Biochem. J.* **277**, 1–10.

Jiao, R., Wu, D., Zhang, B., Cai, S., and Zhai, Z. (1991) Immunogold labelling of the intermediate filament–lamina–nuclear matrix system in HeLa and BHK-21 cells. *J. Electron Microsc. Tech.* **18**, 126–134.

Kao, C. C. (1980) Spinal cord cavitation after injury, *in* Windle,

W. F. (Ed.), The Spinal Cord and its Reaction to Traumatic Injury, pp. 249–270, Marcel Dekker, New York, Basel.

Kao, C. C., and Chang, L. W. (1977) The mechanism of spinal cord cavitation following spinal cord transection, part 1. A correlated histochemical study. *J. Neurosurg.* **46**, 197–209.

Karschin, A., Wassle, H., and Schnitzer, J. (1986) Immunocytochemical studies on astroglia of the cat retina under normal and pathological conditions. *J. Comp. Neurol.* **249**, 564–576.

Kerns, J. M., and Hinsman, E. J. (1973) Neuroglial response to sciatic neurectomy. II. Electron microscopy. *J. Comp. Neurol.* **151**, 255–280.

Kivela, T., Tarkkanen, A., and Virtanen, I. (1986) Intermediate filament in the human retina and retinoblastoma. An immunohistochemical study of vimentin, glial fibrillary acidic protein and neurofilaments. *Invest. Ophthalmol. Visual Sci.* **27**, 1075–1084.

Lawrence, J. B., and Singer, R. H. (1986) Intracellular localization of messenger RNAs for cytoskeletal proteins. *Cell* **45**, 407–415.

Lazarides, E. (1982) Intermediate filaments: A chemically heterogeneous, developmentally regulated class of proteins. *Annu. Rev. Biochem.* **51**, 219–250.

Lendahl, U., Zimmerman, L. B., and McKay, R. D. G. (1990) CNS stem cells express a new class of intermediate filament protein. *Cell* **60**, 585–595.

Lenk, R., Ransom, L., Kaufmann, Y., and Penman, S. (1977) A cytoskeletal structure with associated polyribosomes obtained from HeLa cells. *Cell* **10**, 67–78.

Lewis, G. P., Erickson, P. A., Guerin, C. J., Anderson, D. H., and Fisher, S. K. (1989) Changes in the expression of specific Müller cell proteins during long-term retinal detachment. *Exp. Eye Res.* **49**, 93–111.

Lewis, S. A., Balcarek, J. M., Krek, V., Shelanski, M., and Cowan, N. J. (1984) Sequence of a cDNA clone encoding mouse glial fibrillary acidic protein: Structural conservation of intermediate filaments. *Proc. Natl. Acad. Sci. USA* **81**, 2743–2746.

Maniatis, T., Fritsch, E. F., and Sambrook, J. (1982) Molecular Cloning: A Laboratory Manual, p. 468, Cold Spring Harbor Laboratory, Cold Spring Harbor, NY.

Miller, N. M., and Oberdorfer, M. (1981) Neuronal and neuroglial responses following retinal lesions in the neonatal rats. *J. Comp. Neurol.* **202**, 493–504.

Morrison, R. S., DeVellis, J., Lee, Y.-L., Bradshaw, R. A., and Eng, L. F. (1985) Hormone and growth factors induce the synthesis of glial fibrillary acidic protein in rat brain astrocytes. *J. Neurosci. Res.* **14**, 167–176.

Noller, H. F. (1984) The Structure of Ribosomal RNA. *Annu. Rev. Biochem.* **53**, 119–162.

O'Dowd, D. K., and Eng, L. F. (1979) Immunocytochemical localization of the glial fibrillary acidic (GFA) protein in the Müller cells of the human retina. *Soc. Neurosci. Abstr.* **5**, 431.

Ohira, A., Oshima, K., and Kikuchi, M. (1984) Localization of glial fibrillary acidic (GFA) protein in the human Müller cell. *Nippon Ganka Gakkai Zasshi* **88**, 1068–1074.

Okada, M., Matsumura, M., Yoshimura, N., and Ogino, N. (1988) Human Müller cells express glial fibrillary acidic protein in proliferative vitreoretinopathy. *Invest. Ophthalmol. Visual Sci. (Suppl)* **29**, 305.

Perraud, F., Labourdette, G., Miehe, M., Loret, C., and Sensenbrenner, M. (1988) Comparison of the morphological effects of acidic and basic fibroblast growth factors on rat astroblasts in culture. *J. Neurosci. Res.* **20**, 1–11.

Sarthy, P. V., and Fu, M. (1989a) Transcriptional activation of an intermediate filament protein gene in mice with retinal dystrophy. *DNA* **8**, 437–446.

Sarthy, P. V., Fu, M., and Huang, J. (1989b) Subcellular localization of an intermediate filament protein and its mRNA in glial cells. *Mol. Cell. Biol.* **9**, 4556–4559.

Schroder, H. C., Diehl-Seifert, B., Rottmann, M., Messer, R., Bryson, B. A., Agutter, P. S., and Müller, W. E. G. (1988) Functional dissection of nuclear envelope mRNA translocation system: Effects of phorbol ester and a monoclonal antibody recognizing cytoskeletal structures. *Arch. Biochem. Biophys.* **261**, 394–404.

Schroder, H. C., Rottmann, M., Wenger, R., Bachmann, M., Dorn, A., and Müller, W. E. G. (1987) Studies on protein kinases involved in regulation of nucleocytoplasmic mRNA transport. *Biochem. J.* **252**, 777–790.

Schumm, D. E., and Webb, T. E. (1985) Regulation of RNA transport by cytoplasmic factors. *UCLA Symp. Mol. Cell. Biol.* **26**, 483–506.

Shaw, G., and Weber, K. (1983) The structure and development of the rat retina: An immunofluorescence microscopical study using antibodies specific for intermediate filament proteins. *Eur. J. Cell Biol.* **30**, 219–232.

Silverton, E. W., Navia, M. A., and Davies, D. R. (1977) Three-dimensional structure of an intact human immunoglobulin. *Proc. Natl. Acad. Sci. USA* **74**, 5140–5144.

Singer, R. H., Langevin, G. L., and Lawrence, J. B. (1989) Ultrastructural visualization of cytoskeletal mRNAs and their associated proteins using double-label *in situ* hybridization. *J. Cell Biol.* **108**, 2343–2353.

Steinert, P. M., and Roop, D. R. (1988) Molecular and cellular biology of intermediate filaments. *Annu. Rev. Biochem.* **57**, 593–625.

Stone, J., and Dreher, Z. (1987) Relationship between astrocytes, ganglion cells, and vasculature of the retina. *J. Comp. Neurol.* **255**, 35–49.

Tokuyasu, K. T., Maher, P. A., Dutton, A. H., and Singer, S. J. (1985) Intermediate filaments in skeletal and cardiac muscle tissue in embryonic and adult chicken. *Ann. NY Acad. Sci.* **455**, 200–212.

Traub, P. (1985) Intermediate Filaments, A Review. Springer-Verlag, Berlin.

Trimmer, P. A., Reier, P. J., Oh, T. H., and Eng, L. F. (1982) An ultrastructural and immunocytochemical study of astrocyte differentiation *in vitro:* Changes in the composition and distribution of the cellular cytoskeleton. *J. Neuroimmunol.* **2**, 235–260.

Trimmer, P. A., Phillips, L. L., and Steward, O. (1991) Combination of *in situ* hybridization and immunocytochemistry to detect messenger RNAs in identified CNS neurons and glia in tissue culture. *J. Histochem. Cytochem.* **39**, 891–898.

van Venrooij, W. J., Sillekens, P. G., van Eekelen, C. A. G., and Reinders, R. J. (1981) On the association of mRNA with the cytoskeleton in uninfected and adenovirus-infected human KB cells. *Exp. Cell Res.* **135**, 79–91.

Vaughan, D. K., Erickson, P. A., and Fisher, S. K. (1990) Glial fibrillary acidic protein (GFAP) immunoreactivity in rabbit retina: Effect of fixation. *Invest. Ophthalmol. Visual Sci.* **50**, 385–392.

Walter, P., and Blobel, G. (1982) Signal recognition particle contains a 7S RNA essential for protein translocation across the endoplasmic reticulum. *Nature* **299**, 691–698.

Wang, E. (1985) Intermediate filament associated proteins. *Ann. NY Acad. Sci.* **455**, 32–56.

Weber, P. C., Ohlendorf, D. H., Wendoloski, J. J., and Salemme,

F. R. (1989) Structural origins of high-affinity biotin binding to streptavidin. *Science* **243**, 85–88.

Wolber, R. A., and Beals, T. (1989) Streptavidin–gold labeling for ultrastructural *in situ* nucleic acid hybridization, *in* Hyatt, M. A. (Ed.), Colloidal Gold: Principles, Methods, and Applications, Vol. 2, pp. 379–396, Academic Press, San Diego, CA.

Wolosewick, J. J., and Porter, K. R. (1979) Microtrabecular lattice of the cytoplasmic ground substance. *J. Cell Biol.* **82**, 114–139.

Zorn, T. M. T., de Oliveira, S. F., and Abrahamsohn, P. A. (1990) Organization of intermediate filaments and their association with collagen-containing phagosomes in mouse decidual cells. *J. Struct. Biol.* **103**, 23–33.

Zumbe, A., Stahli, C., and Trachsel, H. (1982) Association of a M_r 50,000 cap-binding protein with the cytoskeleton in baby hamster kidney cells. *Proc. Natl. Acad. Sci. USA* **79**, 2927–2931.

Zumbe, A., and Trachsel, H. (1980) Cap binding protein is associated with a filamentous network. *Eur. J. Cell Biol.* **22**, 376.